J. Fluid Mech. (1982), *vol.* 114, *pp.* 379-398
Printed in Great Britain

Contaminant dispersion in oscillatory flows

By RONALD SMITH

Department of Applied Mathematics and Theoretical Physics,
University of Cambridge, Silver Street, Cambridge CB3 9EW

(Received 2 February 1981)

If the time scale for cross-sectional mixing is comparable with or larger than the flow period, then, after each flow reversal, there can be a substantial time span in which the contaminant cloud is contracting. Thus, the apparent longitudinal-diffusion coefficient is negative. This means that the contaminant dispersion cannot be modelled by a diffusion equation, because negative diffusivities imply the spontaneous development of infinite concentrations. Here it is shown how this periodic contracting and expanding can be modelled by a delay-diffusion equation (Smith 1981)

$$\partial_t \bar{c} + \bar{u}\,\partial_x \bar{c} = \bar{\kappa}\,\partial_x^2 \bar{c} + \int_0^\infty \partial_\tau D\,\partial_x^2 \bar{c}(x - X, t - \tau)\,d\tau,$$

where $\bar{u}(t)$ is the bulk velocity, $X(t,\tau)$ a coordinate displacement, and $D(t,\tau)$ the diffusion coefficient at time τ after discharge. The recent memory $\partial_\tau D$ is always positive and diffusive in character, so singularities cannot arise. However, when τ is large this memory function can be negative because of reversed flow at earlier times. Particular attention is given to estuarial flows and results are derived for the dependence of D upon the water depth and upon the width of the estuary.

1. Introduction

In shear flows the apparent longitudinal diffusivity can exceed molecular or turbulent diffusivities by many orders of magnitude. For example, in the Missouri River, Yotsukura, Fischer & Sayre (1970) measured longitudinal diffusion coefficients in excess of $10^3\ \mathrm{m^2\ s^{-1}}$. If such huge diffusivities were achieved immediately, then a droplet of dye would appear to explode out to a length of 10 metres in less than a tenth of a second. What does happen is that, as the cloud of dye grows across the flow, it experiences more of the velocity shear and is stretched out at a continually increasing rate. The extremely high apparent diffusivities are only achieved after the cloud has been mixed right across the flow.

For oscillatory flows the possibility arises that the flow may have changed direction before the dispersion process has had time to become fully effective. The obvious implication is that the apparent diffusivities are greatly reduced as compared with the corresponding steady flows. For estuaries this sudden drop-off in the value of the longitudinal-diffusion coefficient takes place when the width reaches about 200 m (Holley, Harleman & Fischer 1970). Many major tidal waterways are of just this sort of width. For blood flow, the critical internal diameter for the blood vessels is about 2 mm (Chatwin 1975). Dispersion is fully effective for the smaller capillaries and arterioles, but is seriously inhibited in the larger arteries.

Most previous work (e.g. Aris 1960) has concentrated upon the long-term properties of the dispersion. However, Chatwin (1975) has shown that there can be strong oscillatory effects which dominate the character of the contaminant cloud over time intervals of many periods. Indeed, he points out that the amplitude of the modulation may be such that the contaminant cloud appears to be periodically expanding and contracting: stretched out in the faster parts of the flow in one half-cycle and then returned to only slightly larger than the original shape on the second half-cycle. For estuary flows such contraction after flow reversal is particularly marked (see figure 4 of Holley *et al.* 1970).

Unfortunately, the most commonly used mathematical model for contaminant dispersion is a diffusion equation

$$\partial_t \bar{c} + \bar{u}(t)\,\partial_x \bar{c} = [\bar{\kappa}(t) + D(t,\tau)]\,\partial_x^2 \bar{c} \tag{1.1}$$

(Gill & Sankarasubramanian 1971). Here $\bar{c}(x,t)$ is the cross-sectionally averaged concentration, $\bar{u}$ the bulk velocity, $\bar{\kappa}$ the longitudinal diffusivity, D the shear-dispersion coefficient, and τ the time that has elapsed since discharge. The growth rate of the variance of the contaminant cloud is $2(\bar{\kappa} + D)$. Thus, if the cloud is contracting, then the dispersion coefficient is negative. This has the disastrous implication that singularities (i.e. infinite concentrations) would arise spontaneously (Posmentier 1977).

Many authors (Chatwin 1970; Thacker 1976; Smith 1979) have pointed out that the diffusion equation (1.1) is inappropriate except at very long times after discharge. The principal reason is that the present rate of dispersion depends on how the contaminant has been mixed across the flow further upstream at earlier times (i.e. the concentration variations across the flows are not determined by the local longitudinal concentration gradient). For steady flows, the author (Smith 1981) has recently proposed an alternative model equation in which the dispersion term $D(t,\tau)\,\partial_x^2 \bar{c}$ is replaced by an advected memory term. Here the mathematical analysis is extended to incorporate unsteady flows. The resulting delay-diffusion equation takes the form

$$\partial_t \bar{c} + \bar{u}\,\partial_x \bar{c} = \bar{\kappa}\,\partial_x^2 \bar{c} + \int_0^\infty \partial_\tau D\,\partial_x^2 \bar{c}(x - X, t - \tau)\,d\tau, \tag{1.2}$$

where $X(t,\tau)$ is a co-ordinate displacement. Near $\tau = 0$ the memory function $\partial_\tau D$ is always positive and diffusive in character. However, when τ is large this memory function can be negative because of reversed flow at earlier times. In this way the absence of spontaneous singularities is made compatible with the contraction of the contaminant cloud after flow reversal.

2. Representation of the concentration variations

In principle we are seeking a solution $c(x,y,z,t)$ of the unsteady advection–diffusion equation

$$\left.\begin{aligned} &\partial_t c + u\,\partial_x c - \nabla.(\kappa \nabla c) - \kappa\,\partial_x^2 c = \bar{q}, \\ \text{with}\quad &\kappa \mathbf{n}.\nabla c = 0 \quad \text{on } \partial A, \quad c = 0 \quad \text{at} \quad t = 0. \end{aligned}\right\} \tag{2.1}$$

Here $u(y,z,t)$ is the longitudinal velocity, $\kappa(y,z,t)$ the diffusivity, $\bar{q}(x,t)$ a source term, ∇ the transverse gradient operator $(0, \partial_y, \partial_z)$, ∂A the flow boundary, and $\mathbf{n}$ the outward normal.

The complexity of this equation forces us to seek some simplifications. In the one-dimensional-diffusion approximation (Taylor 1953) it is assumed that

$$c(x,y,z,t) = \bar{c}(x,t) + f(y,z,t)\,\partial_x \bar{c}(x,t) + \dots . \tag{2.2}$$

While this is adequate at large times after discharge, it is not physically sound at earlier stages before the dispersion process has reached its asymptotic state. Instead, we relate the concentration variations across the flow to the bulk properties upstream at earlier times (Smith 1981):

$$c - \bar{c} = \sum_{j=1}^{\infty} \int_0^{\infty} l_j(y,z,t,\tau)\,\partial_x^j \bar{c}(x - X(t,\tau), t-\tau)\,d\tau. \tag{2.3}$$

If we substitute this representation (2.3) into the full equations (2.1) and take the cross-sectional-average value, then we obtain the longitudinal-dispersion equation

$$\partial_t \bar{c} + \bar{u}(t)\,\partial_x \bar{c} - \bar{\kappa}(t)\,\partial_x^2 \bar{c} - \sum_{j=0}^{\infty} \int_0^{\infty} M_j(t,\tau)\,\partial_x^{j+1} \bar{c}(x - X(t,\tau), t-\tau)\,d\tau = \bar{q}, \tag{2.4}$$

with

$$M_1 = \partial_\tau D = \overline{(\bar{u}-u)\,l_1}, \quad M_j = \overline{(\bar{u}-u)\,l_j} + \overline{(\kappa - \bar{\kappa})\,l_{j-1}}. \tag{2.5}$$

Truncation at the second-derivative term gives the delay-diffusion equation (1.2).

Proceeding as in Smith (1981), we find from the $\partial_x^j \bar{c}$ terms in (2.1) that the auxiliary functions $l_j(y,z,t,\tau)$ must satisfy the transverse dispersion equations

$$\left.\begin{aligned} &\partial_t l_1 + \partial_\tau l_1 - \nabla.(\kappa \nabla l_1) = 0, \\ &\text{with} \\ &\kappa \mathbf{n}.\nabla l_1 = 0 \quad \text{on } \partial A, \quad l_1 = \bar{u} - u \quad \text{at} \quad \tau = 0, \end{aligned}\right\} \tag{2.6}$$

$$\left.\begin{aligned} &\partial_t l_2 + \partial_\tau l_2 - \nabla.(\kappa \nabla l_2) = [\partial_\tau X + \partial_t X]\,l_1 + \overline{u l_1} - u l_1, \\ &\text{with} \\ &\kappa \mathbf{n}.\nabla l_2 = 0 \quad \text{on } \partial A, \quad l_2 = \kappa - \bar{\kappa} \quad \text{at} \quad \tau = 0, \end{aligned}\right\} \tag{2.7}$$

$$\left.\begin{aligned} &\partial_t l_j + \partial_\tau l_j - \nabla.(\kappa \nabla l_j) = [\partial_\tau X + \partial_t X]\,l_{j-1} + \overline{u l_{j-1}} - u l_{j-1} + \kappa l_{j-2} - \overline{\kappa l_{j-2}}, \\ &\text{with} \\ &\kappa \mathbf{n}.\nabla l_j = 0 \quad \text{on } \partial A, \quad l_j = 0 \quad \text{at} \quad \tau = 0. \end{aligned}\right\} \tag{2.8}$$

Thus, in the familiar manner of series expansions, we have eliminated any dependence upon the x-co-ordinate at the expense of generating an infinite sequence of lower-dimensional problems for the coefficients l_j. The advantages are that the individual equations (2.6)–(2.8) are easier to solve than the original problem (2.1), and that useful results can be obtained even with a one-term truncation (1.2) (see the remarks at the end of § 4).

3. Memory function

In general, the time dependence of $\kappa(y,z,t)$ precludes us from obtaining explicit analytic solutions to (2.6)–(2.8). However, with an eye towards the problem of dispersion in shallow estuaries, we make the assumption that κ remains spatially self-similar. It then becomes possible to adapt the author's steady-flow results (Smith 1981) with only minor modifications. Of course, in laminar flows κ is constant, and our assumption is trivially satisfied.

Using angle brackets $\langle \ldots \rangle$ to denote time-averaging, we introduce the eigenfunctions $\{\psi_m(y,z)\}$:

$$\left.\begin{aligned} \nabla.(\langle\kappa\rangle \nabla\psi_m) + \lambda_m \psi_m = 0, \\ \langle\kappa\rangle \mathbf{n}.\nabla\psi_m = 0 \quad \text{on } \partial A. \end{aligned}\right\} \tag{3.1}$$

with

For algebraic convenience we shall assume that the modes are normalized:

$$\psi_0 = 1, \quad \overline{\psi_m^2} = 1. \tag{3.2}$$

To represent the starting conditions for $l_1(y,z,t,\tau)$ at $\tau = 0$, we introduce the coefficients

$$u_m(t) = \overline{u\psi_m}, \quad \text{i.e.} \quad u(y,z,t) = \bar{u}(t) + \sum_{m=1}^{\infty} u_m(t)\,\psi_m(y,z). \tag{3.3}$$

The solution for l_1 can then be written

$$l_1 = -\sum_{m=1}^{\infty} u_m(t-\tau)\exp(-\lambda_m I(t,\tau))\,\psi_m(y,z), \tag{3.4}$$

with

$$I(t,\tau) = \int_0^{\tau} (\kappa(t-\tau')/\langle\kappa\rangle)\,d\tau'. \tag{3.5}$$

Also, in terms of u_m the principal memory function $\partial_\tau D$ is given by the neat formula

$$\partial_\tau D = M_1(t,\tau) = \sum_{m=1}^{\infty} u_m(t)\,u_m(t-\tau)\exp(-\lambda_m I(t,\tau)). \tag{3.6}$$

For small τ all the coefficients in the series (3.6) are positive and so $\partial_\tau D$ is positive. However, if the flow is oscillatory, then at large time separation the memory can be negative. In particular, if the flow is sinusoidal,

$$u_m = \alpha_m U \sin(\omega t + \theta_m) \tag{3.7}$$

with κ constant, then we have

$$\begin{aligned} \partial_\tau D &= U^2 \sum_{m=1}^{\infty} \alpha_m^2 \sin(\omega t + \theta_m)\sin(\omega t - \omega\tau + \theta_m)\exp(-\lambda_m\tau) \\ &= \tfrac{1}{2}U^2 \cos\omega\tau \sum_{m=1}^{\infty} \alpha_m^2[1 - \cos 2(\omega t + \theta_m)]\exp(-\lambda_m\tau) \\ &\quad - \tfrac{1}{2}U^2 \sin\omega\tau \sum_{m=1}^{\infty} \alpha_m^2 \sin 2(\omega t + \theta_m)\exp(-\lambda_m\tau). \end{aligned} \tag{3.8}$$

Hence $\partial_\tau D$ is oscillatory with respect to τ, with exponentially decaying amplitude.

Integrating with respect to τ, we obtain the formula

$$\begin{aligned} D(t,\tau) = \tfrac{1}{2}U^2 \sum_{m=1}^{\infty} \frac{\alpha_m^2 \lambda_m}{\omega^2 + \lambda_m^2} \Bigg\{ & 1 - \cos 2(\omega t + \theta_m) - \frac{\omega}{\lambda_m}\sin 2(\omega t + \theta_m) \\ & - 2\exp(-\lambda_m\tau)\sin(\omega t + \theta_m)\left[\sin(\omega t - \omega\tau + \theta_m) - \frac{\omega}{\lambda_m}\cos(\omega t - \omega\tau + \theta_m)\right]\Bigg\}. \end{aligned} \tag{3.9}$$

The constant term agrees with the work of Holley *et al.* (1970), while the non-decaying oscillatory term agrees with the work of Chatwin (1975). A new feature of (3.9) is the explicit dependence upon the time lapse τ since discharge.

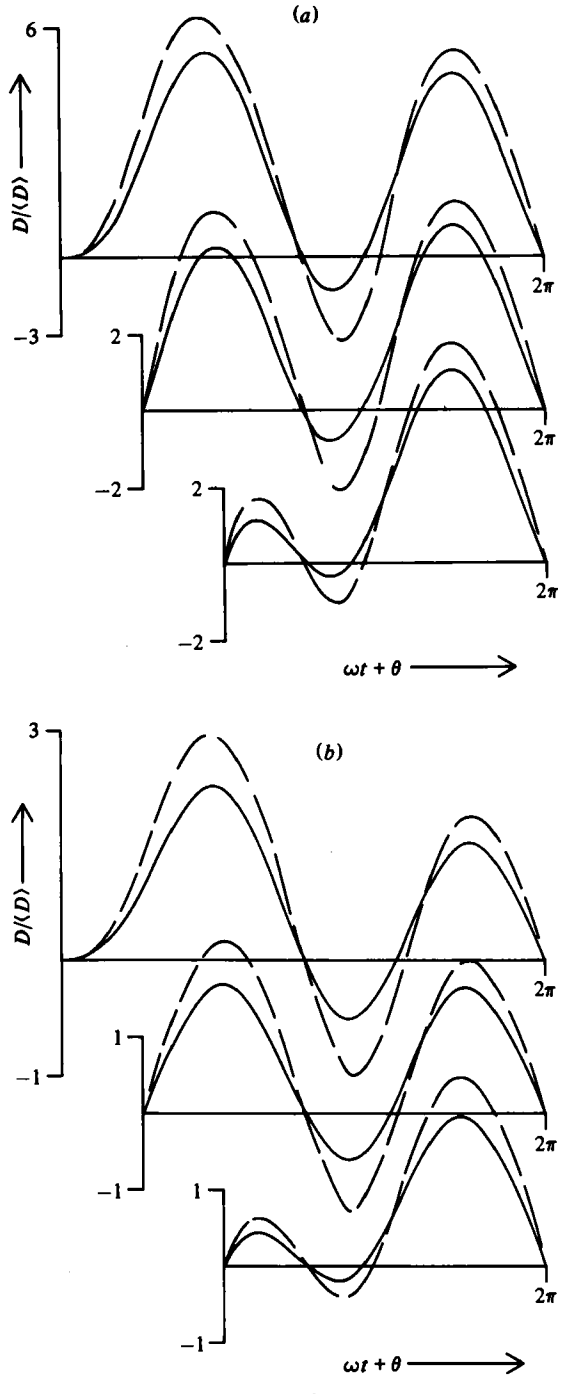

FIGURE 1(*a*, *b*). For legend see page 384.

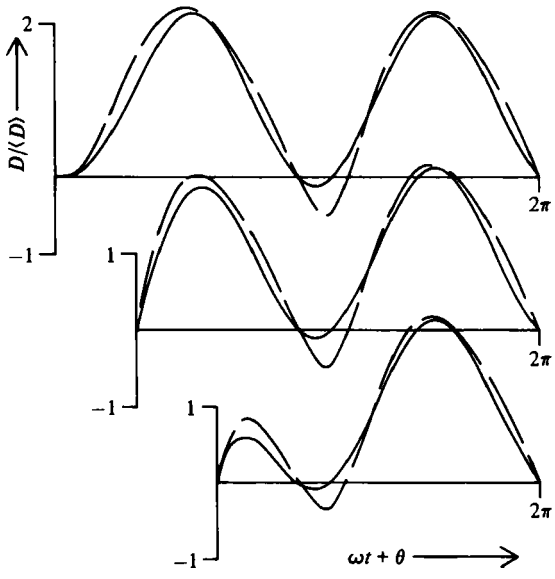

FIGURE 1. Single-mode contribution to the longitudinal-dispersion coefficient for discharges at different times in a sinusoidal flow. (*a*) $\lambda/\omega = 0{\cdot}5$, (*b*) $\lambda/\omega = 1{\cdot}0$, (*c*) $\lambda/\omega = 2$.

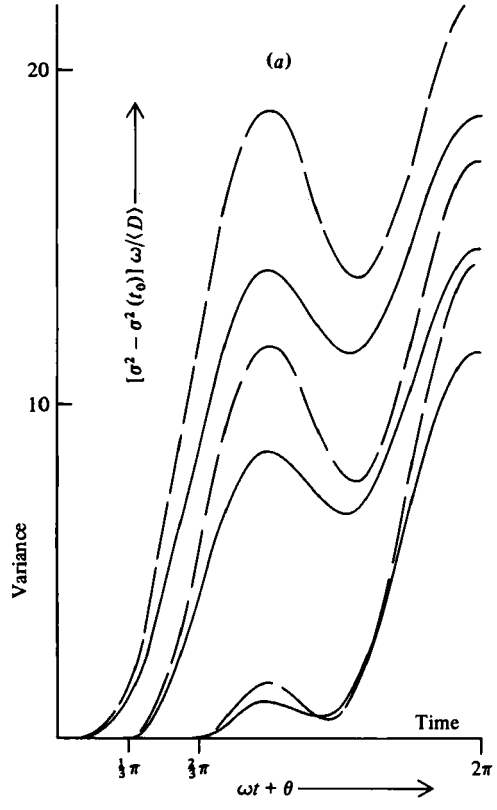

FIGURE 2(*a*). For legend see facing page.

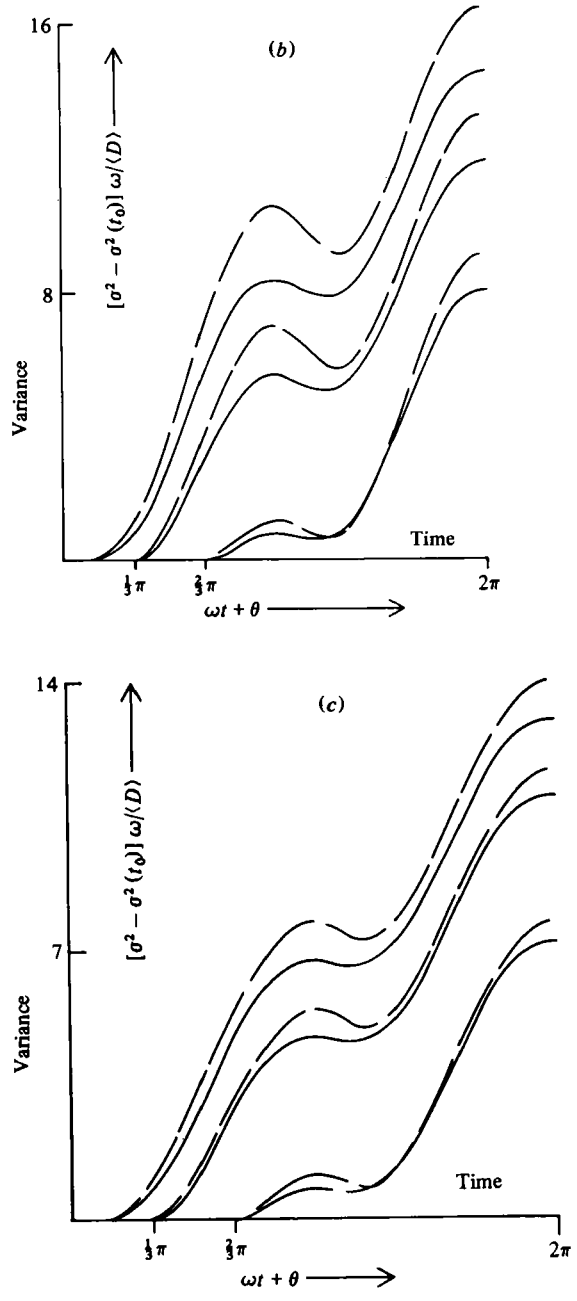

FIGURE 2. Single-mode contribution to the variance for discharges at different times in a sinusoidal flow. (*a*) $\lambda/\omega = 0{\cdot}5$, (*b*) $\lambda/\omega = 1$, (*c*) $\lambda/\omega = 2$.

The greatest contribution to the shear dispersion comes from the mode with λ_m in the vicinity of ω. Thus, a reasonable impression of the time dependence of $D(t,\tau)$ can be obtained from the terms in the curly brackets $\{\ldots\}$. Figures 1(*a*, *b*, *c*) show results for $\lambda_m/\omega = \frac{1}{2}, 1, 2$ and for several different discharge times. In all cases there is a span of time following flow reversal when the contribution to D is negative. As

was remarked in § 1, negative values of D preclude the use of a diffusion description of the concentration distribution.

In practice the measured quantity is the standard deviation for a sudden discharge. Thus, we integrate yet again:

$$\begin{aligned}\sigma^2-\sigma^2(t_0)-2\bar{\kappa}(t-t_0) &= 2\int_0^{t-t_0} D(t_0+\tau,\tau)\,d\tau \\ &= U^2\sum_{m=1}^{\infty}\frac{\alpha_m^2}{\omega^2+\lambda_m^2}\Big\{\lambda_m(t-t_0)-\frac{\lambda_m^2-\omega^2}{\lambda_m^2+\omega^2}+\tfrac{1}{2}\cos 2(\omega t+\theta_m) \\ &\quad+\tfrac{1}{2}\cos 2(\omega t_0+\theta_m)-\frac{1}{2}\frac{\lambda_m}{\omega}\sin 2(\omega t+\theta_m)+\frac{1}{2}\frac{\lambda_m}{\omega}\sin 2(\omega t_0+\theta_m) \\ &\quad+2\frac{\exp(-\lambda_m\tau)}{\omega^2+\lambda_m^2}[\lambda_m\sin(\omega t_0+\theta_m)-\omega\cos(\omega t_0+\theta_m)] \\ &\quad\times[\lambda_m\sin(\omega t+\theta_m)+\omega\cos(\omega t+\theta_m)]\Big\}. \end{aligned} \tag{3.10}$$

Figures 2(*a*, *b*, *c*) show the single-mode contributions to the standard deviation. Qualitatively, these resemble the numerical results obtained by Holley *et al.* (1970, figure 4), and by Allen (1981).

If, as is the case in turbulent flows (Maxey 1978, chap. 3), the diffusivity varies with time, then there are slight changes in the time development of $D(t,\tau)$ and $\sigma^2(t,\tau)$. An extreme case is that of shallow estuaries where the turbulent intensity is proportional to the tidal current

$$\kappa/\langle\kappa\rangle = \tfrac{1}{2}\pi\,|\sin(\omega t+\theta)|. \tag{3.11}$$

The dashed curves in figures 1 and 2 show the results for this case. The general features, of strong oscillations and of negative diffusion after flow reversal, are very much in accord with the constant-κ results.

4. Co-ordinate displacement

The non-homogeneous terms in (2.7) lead us to introduce the further notation

$$\kappa_m(t)=\overline{\kappa\psi_m},\quad u_{mn}(t)=\overline{u\psi_m\psi_n}=\bar{u}\overline{\psi_m\psi_n}+\sum_{j=1}^{\infty}u_j\overline{\psi_j\psi_m\psi_n}. \tag{4.1}$$

The ψ_m coefficient l_{m2} in the eigenfunction expansion for l_2 satisfies the equation

$$\left.\begin{aligned}&(\partial_t+\partial_\tau)\,l_{m2}+\lambda_m\frac{\kappa}{\langle\kappa\rangle}l_{m2}=[\partial_t X+\partial_\tau X-u_{mm}]\,l_{m1}-\sum_{n\neq m}u_{mn}l_{n1},\\ &\text{with}\qquad l_{m2}=\kappa_m(t)\quad\text{at}\quad\tau=0.\end{aligned}\right\} \tag{4.2}$$

The solution is given by

$$\begin{aligned}l_{m2} &= \exp(-\lambda_m I(t,\tau))\Big\{\kappa_m(t-\tau)+u_m(t-\tau)\Big[\int_0^{\tau}u_{mm}(t-\tau')\,d\tau'-X\Big] \\ &\quad+\sum_{n\neq m}u_n(t-\tau)\int_0^{\tau}u_{mn}(t-\tau')\exp(-(\lambda_n-\lambda_m)\,I(t-\tau',\tau-\tau'))\,d\tau'\Big\}. \end{aligned} \tag{4.3}$$

Substituting this result for l_{m2} into (2.5), we find that the second memory function $M_2(t,\tau)$ is given by

$$\begin{aligned} M_2 = &- \sum_{m=1}^{\infty} \exp(-\lambda_m I(t,\tau))\,[\kappa_m(t-\tau)\,u_m(t) + \kappa_m(t)\,u_m(t-\tau)] \\ &+ X(t,\tau)\,M_1(t,\tau) - \sum_{m=1}^{\infty} \exp(-\lambda_m I(t,\tau))\,u_m(t)\,u_m(t-\tau)\int_0^{\tau} u_{mm}(t-\tau')\,d\tau' \\ &- \sum_{m=1}^{\infty} \exp(-\lambda_m I(t,\tau))\,u_m(t) \sum_{n\neq m} u_n(t-\tau)\int_0^{\tau} u_{mn}(t-\tau') \\ &\qquad \times \exp[-(\lambda_n-\lambda_m)\,I(t-\tau',\tau-\tau')]\,d\tau'. \end{aligned} \tag{4.4}$$

The κ_m terms show the effect of the non-uniform longitudinal diffusivity, while the remaining terms give a second approximation to the shear dispersion. In the longitudinal-dispersion equation (2.4) the memory effects are important only if the diffusivity term $\bar{\kappa}(t)$ is small. Thus, for simplicity we shall neglect the diffusive contribution to M_2.

Ideally what we would wish to achieve with our choice of $X(t,\tau)$ is to make the shear contribution to $M_2(t,\tau)$ identically zero. This would ensure that the lowest-order truncation (1.2) of the longitudinal-dispersion equation (2.4) has the accuracy of the next approximation. In general this cannot be achieved because the zeros of $M_1(t,\tau)$ and $M_2(t,\tau)$ do not coincide. An important special case in which this is possible is for shallow estuaries, where all the coefficients $\bar{u}$, u_n, u_{mn} are phase-locked with each other. The optimal choice for $X(t,\tau)$ is then

$$\begin{aligned} X(t,\tau) = \frac{1}{M_1(t,\tau)} \sum_{m=1}^{\infty}\sum_{n=1}^{\infty} \Big\{ & u_m(t)\,u_n(t-\tau)\exp(-\lambda_m I(t,\tau)) \\ & \times \int_0^{\tau} u_{mn}(t-\tau')\exp[-(\lambda_n-\lambda_m)\,I(t-\tau',\tau-\tau')]\,d\tau' \Big\}. \end{aligned} \tag{4.5}$$

A simple approximation for $X(t,\tau)$ is to assume that the displacement velocity $\partial_\tau X$ takes the form

$$\left.\begin{aligned} \partial_\tau X &= \bar{u}(t-\tau) + w(t-\tau), \\ \text{i.e.} \qquad X(t,\tau) &= \int_0^{\tau} [\bar{u}(t-\tau') + w(t-\tau')]\,d\tau'. \end{aligned}\right\} \tag{4.6}$$

To define the excess velocity w we choose to eliminate any long-term influence of the second memory function:

$$\int_0^{\infty} M_2(t,\tau)\,d\tau = 0. \tag{4.7}$$

Remarkably, we can sum the double series (4.4) explicitly to obtain an integral equation for w:

$$\int_0^{\infty} w(t-\tau)\int_{\tau}^{\infty} M_1(t,\tau')\,d\tau'\,d\tau = \overline{(u-\bar{u})fg}. \tag{4.8}$$

Here the auxiliary functions g, f satisfy the forwards- and backwards-going diffusion equations

$$\left.\begin{aligned} &\partial_t g - \nabla.(\kappa\nabla g) = u - \bar{u}, \\ \text{with} \qquad &\bar{g} = 0, \quad \kappa\mathbf{n}.\nabla g = 0 \quad \text{on } \partial A, \end{aligned}\right\} \tag{4.9}$$

$$\left.\begin{aligned} -\partial_t f - \nabla.(\kappa \nabla f) &= u - \bar{u}, \\ \bar{f} = 0, \quad \kappa \mathbf{n}.\nabla f &= 0 \quad \text{on } \partial A, \end{aligned}\right\} \tag{4.10}$$

with

where any free transients are assumed to have decayed away.

In passing, we record that, at large times after discharge, in axes moving with the bulk velocity $\bar{u}$, the second and third moments $\bar{c}^{(2)}, \bar{c}^{(3)}$ of the concentration distribution are given by

$$\left.\begin{aligned} \bar{c}^{(2)}/\bar{c}^{(0)} &\sim 2\int_{t_0}^{t} \overline{ug}(t')\,dt' - 2\overline{fg}(t_0), \\ \partial_t \bar{c}^{(3)}/\bar{c}^{(0)} &\sim \overline{6(u-\bar{u})fg}(t). \end{aligned}\right\} \tag{4.11}$$

These are the generalizations to arbitrary unsteady flows of results given by Chatwin (1970, 1975) for steady and for sinusoidal flows. In particular, the above choice (4.8) for the co-ordinate displacement ensures that at large times after discharge the growth rate of the skewness is predicted correctly by the delay-diffusion equation (1.2).

5. Two-layer approximation

An extremely desirable property for a model equation to possess is that it should be exact for some physically meaningful limiting case. This would then guarantee that the solutions are free from gross physical contradictions, such as the spontaneous development of singularities. In this section we follow Thacker (1976) and show that for a two-layer flow the delay-diffusion equation (1.2) is exact.

Let c_+, c_- be the concentrations in two well-mixed layers with relative areas $\frac{1}{2}(1-\xi), \frac{1}{2}(1+\xi)$ and with layer velocities $u_+(t), u_-(t)$ (see figure 3). If $\lambda(t)$ is the exchange rate between the layers, and $q_+(t), q_-(t)$ are the source strengths, then the evolution equations for the contaminant concentrations c_+, c_- take the form

$$\left.\begin{aligned} \partial_t c_+ + u_+ \partial_x c_+ &= \tfrac{1}{2}(1+\xi)\lambda(c_- - c_+) + q_+, \\ \partial_t c_- + u_- \partial_x c_- &= \tfrac{1}{2}(1-\xi)\lambda(c_+ - c_-) + q_-. \end{aligned}\right\} \tag{5.1}$$

For steady flows the characteristic velocities u_+, u_- are constant and the hyperbolic equations (5.1) can be solved analytically (Thacker 1976).

If we introduce the notation

$$\bar{c} = \tfrac{1}{2}(1-\xi)c_+ + \tfrac{1}{2}(1+\xi)c_-, \quad \Delta c = \tfrac{1}{2}(c_+ - c_-), \tag{5.2}$$

to denote the cross-sectional-average values and the departures from the average, then (5.1) can be re-written as

$$\left.\begin{aligned} \partial_t \bar{c} + \bar{u}\partial_x \bar{c} &= \bar{q} - (1-\xi^2)\Delta u \partial_x \Delta c, \\ \partial_t \Delta c + (\bar{u} + 2\xi \Delta u)\partial_x \Delta c + \lambda \Delta c &= \Delta q - \Delta u \partial_x \bar{c}. \end{aligned}\right\} \tag{5.3}$$

When the source distribution is uniform across the flow, the solution for Δc is given by

$$\left.\begin{aligned} \Delta c &= -\int_0^\infty \Delta u(t-\tau) \exp\left(-\int_0^\tau \lambda(t-t')\,dt'\right) \partial_x \bar{c}(x - X, t-\tau)\,d\tau \\ X(t,\tau) &= \int_0^\tau [\bar{u}(t-t') + 2\xi \Delta u(t-t')]\,dt'. \end{aligned}\right\} \tag{5.4}$$

with

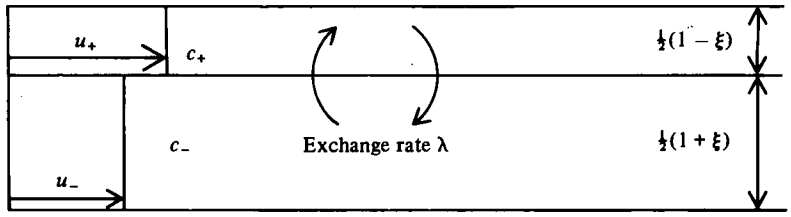

FIGURE 3. Definition sketch for a two-layer flow.

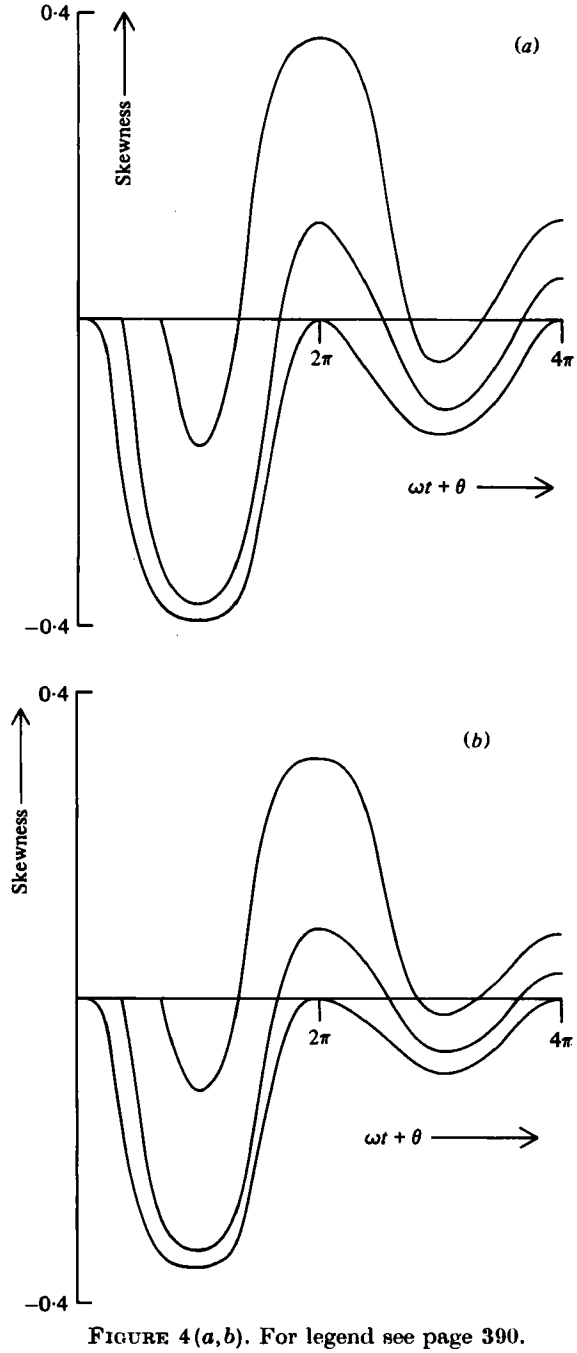

FIGURE 4 (*a*, *b*). For legend see page 390.

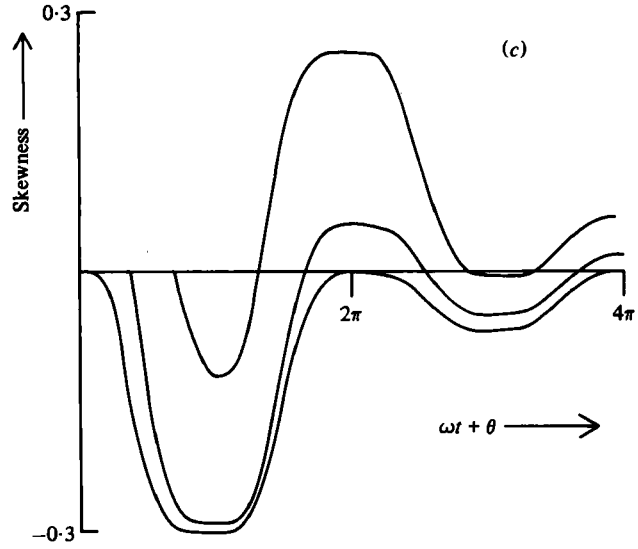

FIGURE 4. Skewness as a function of time for a two-layer sinusoidal flow with $\xi = -7^{\frac{1}{2}}/5$ and $\sigma^2(t_0) = \langle D\rangle/\omega$. For smaller initial variance the skewness would be greater, particularly near $\tau = 0$. (*a*) $\lambda/\omega = 0{\cdot}5$, (*b*) $\lambda/\omega = 1$, (*c*) $\lambda/\omega = 2$.

If this is substituted into the equation for $\bar{c}$ then we obtain the delay-diffusion equation

$$\left.\begin{aligned} &\partial_t \bar{c} + \bar{u}(t)\,\partial_x \bar{c} - \int_0^\infty M_1(t,\tau)\,\partial_x^2 \bar{c}(x-X, t-\tau)\,d\tau = \bar{q}, \\ \text{with}\quad &M_1(t,\tau) = (1-\xi^2)\,\Delta u(t)\,\Delta u(t-\tau)\exp\left(-\int_0^\tau \lambda(t-t')\,dt'\right). \end{aligned}\right\} \tag{5.5}$$

Hence the model equation (1.2) is indeed exact for the two-layer system (5.1).

The skewness of the concentration distribution depends upon the parameter ξ. In particular, if the flow is sinusoidal,

$$(1-\xi^2)^{\frac{1}{2}}\,\Delta u = \alpha U \sin(\omega t + \theta) \tag{5.6}$$

with λ constant, then the standard deviation is given by the one-term version of (3.10), and the third moment $\bar{c}^{(3)}$ is given by

$$\begin{aligned} \bar{c}^{(3)} = \frac{3\xi(\alpha U)^3 \bar{c}^{(0)}}{\omega^2(\omega^2+\lambda^2)(4\omega^2+\lambda^2)[1-\xi^2]^{\frac{1}{2}}} \{ &-3\omega^2\lambda[\sin(\omega t+\theta)+\sin(\omega t_0+\theta)] \\ &+\omega^2\lambda[\sin 3(\omega t+\theta)+\sin 3(\omega t_0+\theta)] \\ &-3\omega(\lambda^2+2\omega^2)[\cos(\omega t+\theta)-\cos(\omega t_0+\theta)] \\ &+\tfrac{1}{3}\omega(\lambda^2-2\omega^2)[\cos 3(\omega t+\theta)-\cos 3(\omega t_0+\theta)] \\ &+2\lambda^2\omega\exp(-\lambda(t-t_0))[\sin 2(\omega t_0+\theta)\sin(\omega t+\theta)-\sin(\omega t_0+\theta)\sin 2(\omega t+\theta)] \\ &+4\omega^3\exp(-\lambda(t-t_0))[\cos(\omega t_0+\theta)\cos 2(\omega t+\theta)-\cos 2(\omega t_0+\theta)\cos(\omega t+\theta)] \\ &+2\lambda\omega^2\exp(-\lambda(t-t_0))[\sin 2(\omega t_0+\theta)\cos(\omega t+\theta)+\sin 2(\omega t+\theta)\cos(\omega t_0+\theta) \\ &-2\sin(\omega t+\theta)\cos 2(\omega t_0+\theta)-2\sin(\omega t_0+\theta)\cos 2(\omega t+\theta)]\}. \end{aligned} \tag{5.7}$$

Unlike the steady flow case (Chatwin 1970), the third moment $\bar{c}^{(3)}$ remains bounded. Thus, the skewness

$$\gamma = \bar{c}^{(3)}/\bar{c}^{(0)}\sigma^3 \tag{5.8}$$

only develops strongly in the first flow oscillation and subsequently fades away at the overall rate $t^{-\frac{3}{2}}$ (see figures 4*a–c*). Again, there is qualitative agreement with the numerical results of Allen (1981). Holley *et al.* (1970) did not calculate the skewness. However, they did remark upon the disparity between the skewed distributions at the half period and the symmetrical distribution at the full period. In their work the discharge was made at the turn of the tide. Thus, the two-layer equation (5.7) would indeed predict zero skewness at every subsequent full period (see figures 4*a*, *b*, *c*).

6. Shallow estuaries

In water depth of 10 m and with friction velocity 0·02 m s^{-1}, the *e*-folding time for vertical mixing is about 600 s (Smith 1979, equation (2.7)). Thus, on a tidal time scale we can ignore vertical concentration variations, and the local longitudinal velocity will be proportion to the bulk velocity $\bar{u}$. Integrating the eigenmode equation (3.1) from $z = -h$ to $z = 0$, we obtain the transverse eigenvalue problem

$$\left.\begin{aligned} &\frac{d}{dy}\left(h\langle\|\kappa\|\rangle\frac{d}{dy}\psi_m\right) + \lambda_m h\psi_m = 0, \\ &h\langle\|\kappa\|\rangle d\psi_m/dy = 0 \quad \text{at} \quad y = y_-, y_+. \end{aligned}\right\} \tag{6.1}$$

with

Here $h(y)$ is the water depth, y_+, y_- are the two sides of the estuary, and $\langle\|\kappa\|\rangle$ denotes the vertically and tidally averaged transverse diffusivity. Similarly, we represent the vertically averaged velocity profile as

$$\|u\| = \bar{u}(t)\left[1 + \sum_{m=1}^{\infty} \alpha_m \psi_m(y)\right]. \tag{6.2}$$

The numerical values of the coefficients α_m, λ_m depend upon the velocity and depth profiles across the estuary. For example, if we assume that

$$\|u\| = \bar{u}h^{\beta-1}\bar{h}/\overline{h^\beta}, \quad \langle\|\kappa\|\rangle = K_2 U\bar{h}h^\gamma/\overline{h^\gamma}, \tag{6.3}$$

then the coefficients are determined by the equations

$$\left.\begin{aligned} &\frac{d}{dy}\left(h^{\gamma+1}\frac{d}{dy}\psi_m\right) + \frac{\lambda_m\overline{h^\gamma}}{K_2 U\bar{h}}h\psi_m = 0, \\ &\frac{1}{y_+ - y_-}\int_{y_-}^{y_+}\frac{h}{\bar{h}}\psi_m^2 dy = 1, \\ &\alpha_m = \frac{1}{y_+ - y_-}\int_{y_-}^{y_+}\frac{h^\beta}{\overline{h^\beta}}\psi_m dy. \end{aligned}\right\} \tag{6.4}$$

Here U is the peak value of $\bar{u}(t)$, and the empirical constant K_2 is about 0·01 (Talbot & Talbot 1974). The most realistic choice for the exponents is to take

$$\beta = \gamma = \tfrac{3}{2} \tag{6.5}$$

(Smith 1976).

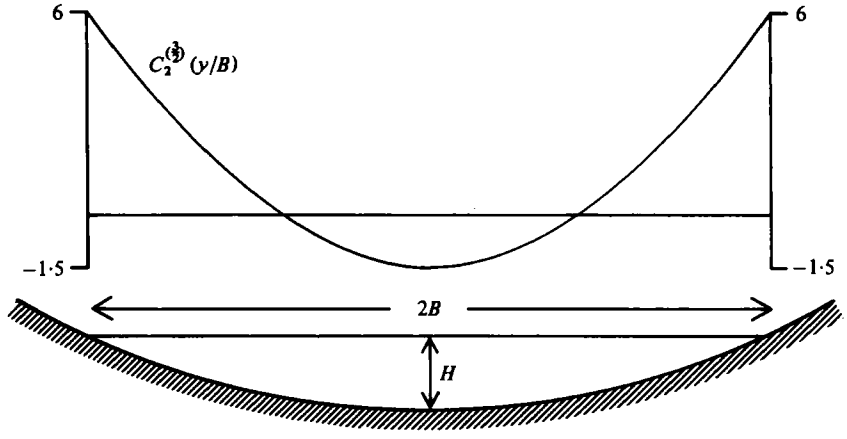

FIGURE 5. Definition sketch for a parabolic estuary.

A model which is analytically convenient, yet is not too dissimilar to the optimal choice of exponents, is

$$\|u\| = \overline{u}h\overline{h}/\overline{h^2}, \quad \langle\|\kappa\|\rangle = K_2 Uh \tag{6.6}$$

(Fischer 1972). In particular, for a parabolic depth profile

$$h(y) = H[1-(y/B)^2] \quad (-B < y < B) \tag{6.7}$$

(see figure 5) the eigenmodes are ultraspherical polynomials:

$$\left.\begin{aligned} \psi_m &= \left[\frac{2(2m+3)}{3(m+1)(m+2)}\right]^{\frac{1}{2}} C_m^{(\frac{3}{2})}(y/B), \\ \lambda_m &= m(m+3)K_2 UH/B^2 \end{aligned}\right\} \tag{6.8}$$

(Abramowitz & Stegun 1965, chap. 22). The crucial feature which makes this example so easy is that the velocity profile involves just the $m = 2$ mode:

$$\left.\begin{aligned} u &= \overline{u}[1-\tfrac{1}{6}C_2^{(\frac{3}{2})}(y/B)], \\ \text{with} \quad C_2^{(\frac{3}{2})} &= \tfrac{15}{2}(y/B)^2 - \tfrac{3}{2}, \\ \text{i.e.} \quad \alpha_2 &= -(\tfrac{1}{14})^{\frac{1}{2}}. \end{aligned}\right\} \tag{6.9}$$

In this circumstance the optimum and asymptotic choices (4.5), (4.8) for the centroid displacement are identical,

$$X(t,\tau) = \int_0^\tau u_{22}(t-\tau')\,d\tau' = \frac{2}{3}\int_0^\tau \overline{u}(t-\tau')\,d\tau'. \tag{6.10}$$

Furthermore, the two-layer approximation (5.3) is exactly equivalent to the delay-diffusion equation (1.2) provided that we choose

$$\left.\begin{aligned} \xi &= -7^{\frac{1}{2}}/5, \quad \Delta u = \frac{5}{7^{\frac{1}{2}}\times 6}\overline{u}, \\ \lambda &= 10(\kappa/\langle\kappa\rangle)K_2 UH/B^2. \end{aligned}\right\} \tag{6.11}$$

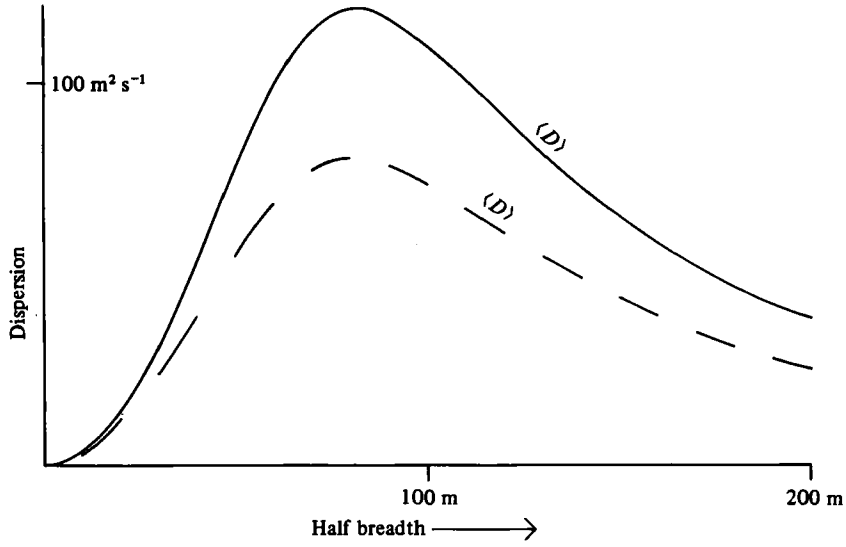

FIGURE 6. Long-term averaged dispersion coefficient for a 10 m deep estuary with peak tidal velocity 1 m s^{-1}.

If we model the turbulence as being steady and the tidal current as being sinusoidal,

$$\bar{u} = U \sin \omega t, \tag{6.12}$$

then at large times after discharge we find that the tidally averaged dispersion coefficient is given by the simple formula

$$\langle D \rangle = \frac{5K_2 U^3 H B^2}{14[\omega^2 B^4 + 100 K_2^2 U^2 H^2]}. \tag{6.13}$$

Figure 6 shows the predicted dispersion coefficient as a function of half-width B for an estuary with maximum depth 10 m, peak velocity 1 m s^{-1}, and semi-diurnal frequency $\omega = 1{\cdot}5 \times 10^{-4}$ s^{-1}. As before, the dashed curve in figure 6 gives the results for the case in which the diffusivity is proportional to the tidal current. There is good overall agreement with the model calculations of Holley *et al.* (1970, equation (23)). To construct the complete time-dependent dispersion coefficient, it is necessary to multiply the above result (6.13) by the time-dependent factor shown in figures 1 (*a–c*).

7. Calculation of the velocity profile

A major obstacle to the study of dispersion in oscillatory flows is the need to know the unsteady non-uniform velocity profile. Assuming that the pressure gradient $-G(t)$ is uniform along and across the flow, then we can write the longitudinal-momentum equation

$$\left.\begin{aligned} &\partial_t u - \nabla.(\nu \nabla u) = G(t), \\ \text{with} \qquad &u = 0 \quad \text{on rigid parts of } \partial A, \\ &\nu \mathbf{n}.\nabla u = 0 \quad \text{on free parts of } \partial A. \end{aligned}\right\} \tag{7.1}$$

The natural eigenmodes $\Phi^{(l)}(y, z)$ satisfy the field equations

$$\nabla.(\langle \nu \rangle \nabla \Phi^{(l)}) + \mu^{(l)} \Phi^{(l)} = 0, \tag{7.2}$$

with the corresponding rigid and free boundary conditions. A suitable normalization is to take

$$\overline{\Phi^{(l)2}} = 1. \tag{7.3}$$

The resulting solution for the velocity field is

$$\left.\begin{aligned} u(y,z,t) &= \sum_{l=0}^{\infty} u^{(l)}(t)\,\Phi^{(l)}(y,z), \\ \text{with} \qquad u^{(l)} &= \int_0^{\infty} \overline{\Phi^{(l)}} G(t-\tau)\exp\left(-\mu^{(l)}J(t,\tau)\right)d\tau, \end{aligned}\right\} \tag{7.4}$$

where by analogy with (3.5) we have defined

$$J(t,\tau) = \int_0^{\tau} [\nu(t-\tau')/\langle\nu\rangle]\,d\tau'. \tag{7.5}$$

If it is the bulk velocity $\bar{u}(t)$ that is externally imposed, then the pressure gradient is determined by the integral equation

$$\int_0^{\infty} G(t-\tau) \sum_{l=0}^{\infty} \overline{(\Phi^{(l)})}^2 \exp\left(-\mu^{(l)}J(t,\tau)\right)d\tau = \bar{u}(t) \tag{7.6}$$

For the eventual dispersion calculation it is necessary to calculate the velocity coefficients $u_m(t)$ with respect to the diffusion eigenmodes $\{\psi_m(y,z)\}$. This involves yet another infinite series:

$$u_m = \sum_{l=0}^{\infty} u^{(l)} \overline{\psi_m \Phi^{(l)}} \quad (m = 1, 2, \ldots). \tag{7.7}$$

The simplicity of the previous example lay in the fact that for shallow estuaries the velocity eigenvalues $\mu^{(l)}$ are so large that the response time for the pressure gradient is extremely rapid, leading to simple proportionality between u_m and $\bar{u}$. Another simple example is studied in § 8.

8. Deep estuaries

For very large estuaries there is little cross-sectional mixing achieved on the time scale of the order of one tidal oscillation. Thus, the transverse oscillatory shear ceases to be the dominant mechanism for longitudinal dispersion. One mechanism which can continue to be important is the oscillatory vertical velocity shear (Bowden 1965; Allen 1981). In this section we give a simple model calculation for the dispersion coefficient associated with this mechanism.

For simplicity we ignore any time dependence of the turbulent structure and we assume that the vertical eddy diffusivities of mass and momentum are equal:

$$\left.\begin{aligned} \kappa = \nu &= \hat{\kappa} h u_* (1-\eta)\,\eta, \\ \text{with} \qquad \eta &= \eta_* + (1+z/h)\,(1-\eta_*). \end{aligned}\right\} \tag{8.1}$$

Here $\hat{\kappa}$ is a dimensionless constant (about 0·4), h is the water depth, u_* a turbulent velocity scale, and η_* a dimensionless roughness height.

Since η_* is usually extremely small (e.g. 2 cm roughness elements in water of depth

20 m), the eigenmodes for velocity and concentration are virtually identical except in the immediate vicinity of the estuary bed. If we relax the normalization (7.3), then correct to order η_* the two classes of eigenmodes are given by

$$\begin{aligned}
\psi_m &= (2m+1)^{\frac{1}{2}} P_m(2\eta-1),\\
\lambda_m &= m(m+1)\,\hat{\kappa}\langle u_*\rangle/h,\\
\Phi^{(l)} &= (2l+1)^{\frac{1}{2}}\Big\{P_l(2\eta-1)\,[1+\ln\eta/(-\ln\eta_*)]\\
&\quad+\frac{2}{-\ln\eta_*}\sum_{j=0}^{l-1}\frac{(-1)^{l-j}(2j+1)}{(l-j)(l+j+1)}P_j(2\eta-1)\\
&\quad-\frac{2}{-\ln\eta_*}P_l(2\eta-1)\sum_{j=0}^{l-1}\frac{2j+1}{(l-j)(l+j+1)}\Big\},\\
\mu^{(l)} &= \frac{\hat{\kappa}\langle u_*\rangle}{h}\{l(l+1)+(2l+1)/(-\ln\eta_*)\},
\end{aligned}\tag{8.2}$$

where P_j is the Legendre polynomial of degree j. The normalization (7.3) is only satisfied to leading order with respect to the small parameter $1/(-\ln\eta_*)$.

Retaining only the dominant terms, we have

$$\overline{\Phi^{(0)}} = 1, \quad \overline{\Phi^{(l)}} = \frac{(-1)^l(2l+1)^{\frac{1}{2}}}{(-\ln\eta_*)\,l(l+1)}.\tag{8.3}$$

Thus, equation (7.6) for the pressure gradient is dominated by the $l=0$ term. The solution for $G(t)$ is

$$G(t) \doteq \partial_t\bar{u}+\kappa\langle u_*\rangle\,\bar{u}(t)\,\nu(t)/[\langle\nu\rangle\,h(-\ln\eta_*)].\tag{8.4}$$

The presence of the small parameter $1/(-\ln\eta_*)$ shows that there can be a significant phase lag between the pressure gradient and the bulk velocity.

The orthogonality of the Legendre polynomials implies that the infinite series (7.7) is dominated by the $l=0$ and $l=m$ terms:

$$u_m \doteq \frac{(-1)^{m+1}(2m+1)^{\frac{1}{2}}}{(-\ln\eta_*)\,m(m+1)}\left\{\bar{u}(t)-\int_0^\infty \partial_t\bar{u}(t-\tau)\exp\left(-\mu^{(m)}J(t,\tau)\right)d\tau\right\}.\tag{8.5}$$

In particular, for a sinusoidal bulk flow

$$\bar{u} = U\sin\omega t,\tag{8.6}$$

with ν independent of time, we have

with
$$\left.\begin{aligned}
u_m &= \alpha_m U\sin(\omega t+\theta_m),\\
\alpha_m &= \frac{(-1)^m(2m+1)^{\frac{1}{2}}\mu^{(m)}}{(-\ln\eta_*)\,m(m+1)\,[\omega^2+\mu^{(m)2}]^{\frac{1}{2}}},\\
\tan\theta_m &= -\omega/\mu^{(m)}.
\end{aligned}\right\}\tag{8.7}$$

If we non-dimensionalize the frequency and define the turbulent velocity scale

$$\Omega = \omega h/\hat{\kappa}\langle u_*\rangle, \quad \langle u_*\rangle = \hat{\kappa}U/(-\ln\eta_*),\tag{8.8}$$

then the formula for the tidally averaged dispersion coefficient can be written

$$\langle D\rangle = \frac{1}{2}\frac{h\langle u_*\rangle}{\hat{\kappa}^3}\sum_{m=1}^{\infty}\frac{(2m+1)\,m(m+1)}{[\Omega^2+m^2(m+1)^2]^2}.\tag{8.9}$$

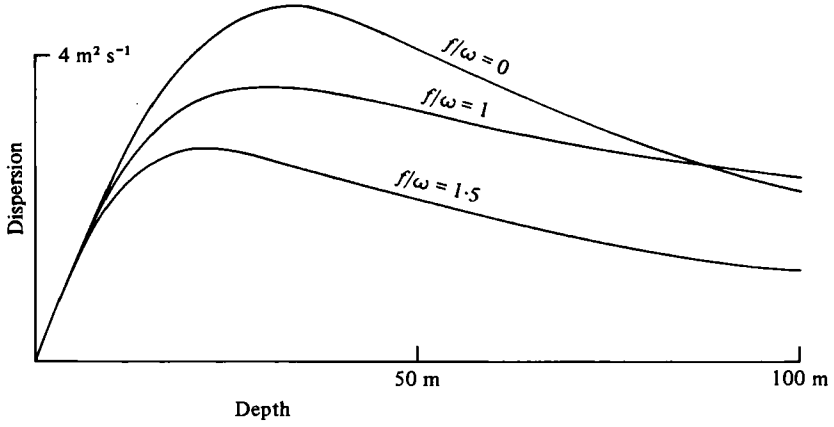

FIGURE 7. Long-term averaged dispersion coefficient for deep water with averaged friction velocity $\langle u_* \rangle = 0{\cdot}04$ m s^{-1}.

This is the oscillatory-flow generalization of the steady-flow result derived by Elder (1959, equation (14)). As deduced by Bowden (1965), for low frequencies the dispersion coefficient is exactly half the steady-state value.

Figure 7 shows the predicted dispersion coefficient as a function of depth h for an estuary with $\langle u_* \rangle = 0{\cdot}04$ m s^{-1}, $\hat{\kappa} = 0{\cdot}4$, and semi-diurnal frequency

$$\omega = 1{\cdot}5 \times 10^{-4} \text{ s}^{-1}.$$

Again, there is good overall agreement with the results of Holley *et al.* (1970) – see Chatwin (1975, figure 1). The present results have the advantages of more faithful representations of the velocity profile and of the turbulence structure. In particular, the phase variations of the current with height (Chatwin 1975, equations (4.6)–(4.8)) are accounted for.

9. Coriolis effect in deep estuaries

One potentially important physical effect, which has thus far been neglected, is the Coriolis deflection (to the right) of the tidal current. Fortunately, its inclusion is quite straightforward provided that we assume the longitudinal and transverse turbulent diffusivities are equal.

Instead of the single momentum equation (7.1), we now have the coupled pair of equations

with

$$\left.\begin{aligned} \partial_t u - fv - \partial_z(\nu \partial_z u) &= G(t), \\ \partial_t v + fu - \partial_z(\nu \partial_z v) &= H(t), \\ u = v &= 0 \quad \text{on} \quad z = -h, \\ \nu \partial_z u = \nu \partial_z v &= 0 \quad \text{on} \quad z = 0. \end{aligned}\right\} \tag{9.1}$$

Here f is the Coriolis frequency, v the velocity across the estuary, and $-H(t)$ the transverse pressure gradient. If we pose the representations

$$u(z,t) = \sum_{l=0}^{\infty} u^{(l)}(t)\, \Phi^{(l)}(z), \quad v(z,t) = \sum_{l=0}^{\infty} v^{(l)}(t)\, \Phi^{(l)}(z), \tag{9.2}$$

then the equations for the coefficients $u^{(l)}, v^{(l)}$ take the form

$$\left.\begin{aligned}\partial_t u^{(l)} + \mu^{(l)} \frac{\nu}{\langle \nu \rangle} u^{(l)} - f v^{(l)} &= \overline{\Phi^{(l)}} G(t), \\ \partial_t v^{(l)} + \mu^{(l)} \frac{\nu}{\langle \nu \rangle} v^{(l)} + f u^{(l)} &= \overline{\Phi^{(l)}} H(t).\end{aligned}\right\} \tag{9.3}$$

In terms of $G(t)$ and $H(t)$ the solution can be written

$$\left.\begin{aligned}u^{(l)} &= \overline{\Phi^{(l)}} \int_0^\infty G(t-\tau) \cos f\tau \exp\left(-\mu^{(l)} J(t,\tau)\right) d\tau \\ &\quad + \overline{\Phi^{(l)}} \int_0^\infty H(t-\tau) \sin f\tau \exp\left(-\mu^{(l)} J(t,\tau)\right) d\tau, \\ v^{(l)} &= -\overline{\Phi^{(l)}} \int_0^\infty G(t-\tau) \sin f\tau \exp\left(-\mu^{(l)} J(t,\tau)\right) d\tau \\ &\quad + \overline{\Phi^{(l)}} \int_0^\infty H(t-\tau) \cos f\tau \exp\left(-\mu^{(l)} J(t,\tau)\right) d\tau,\end{aligned}\right\} \tag{9.4}$$

with $J(t,\tau)$ defined by (7.5).

In practice, it is not the pressure field that is externally imposed, but rather the bulk velocity $\bar{u}(t), \bar{v}(t)$. From (8.3) we infer that the dominant contributions arise from the $l = 0$ mode. Hence we deduce that

$$\left.\begin{aligned}G(t) &\doteq \partial_t \bar{u} + \mu^{(0)} \frac{\nu}{\langle \nu \rangle} \bar{u} - f\bar{v}, \\ H(t) &\doteq \partial_t \bar{v} + \mu^{(0)} \frac{\nu}{\langle \nu \rangle} \bar{v} + f\bar{u}.\end{aligned}\right\} \tag{9.5}$$

An appropriate alignment of the axes with the estuary shape enables us to set $\bar{v} = 0$. The net result is that, instead of (8.5), we now have

$$u_m \doteq \frac{(-1)^{m+1}(2m+1)^{\frac{1}{2}}}{(-\ln \eta_*)\, m(m+1)} \left\{ \bar{u}(t) - \int_0^\infty \partial_t \bar{u}(t-\tau) \cos f\tau \exp\left(-\mu^{(m)} J(t,\tau)\right) d\tau \right. \\ \left. - f \int_0^\infty \bar{u}(t-\tau) \sin f\tau \exp\left(-\mu^{(m)} J(t,\tau)\right) d\tau \right\}. \tag{9.6}$$

For a sinusoidal bulk flow

$$\bar{u} = U \sin \omega t, \tag{9.7}$$

with ν independent of time, we can evaluate the integrals to obtain

$$u_m = \frac{(-1)^{m+1}(2m+1)^{\frac{1}{2}} \mu^{(m)}}{(-\ln \eta_*)\, m(m+1)\, [(\omega+f)^2 + \mu^{(m)2}]\, [(\omega-f)^2 + \mu^{(m)2}]} \\ \times \{\mu^{(m)} [\omega^2 + \mu^{(m)2} + f^2] \sin \omega t - \omega [\omega^2 + \mu^{(m)2} - f^2] \cos \omega t\}. \tag{9.8}$$

If we non-dimensionalize the Coriolis frequency,

$$F = f/\omega,$$

then the formula for the tidally averaged dispersion coefficient becomes

$$\langle D \rangle = \frac{\frac{1}{2} h \langle u_* \rangle}{\hat{\kappa}^3} \sum_{m=1}^{\infty} \frac{(2m+1)\, m(m+1)\, [(m^2(m+1)^2 + \Omega^2(1+F^2))^2 - 4\Omega^4 F^2]}{[\Omega^2(1+F)^2 + m^2(m+1)^2]^2\, [\Omega^2(1-F)^2 + m^2(m+1)^2]^2}. \tag{9.9}$$

Figure 7 reveals that, for sufficiently deep estuaries, the longitudinal-dispersion process is strongly modified by the Earth's rotation.

I wish to thank British Petroleum and the Royal Society for financial support.

REFERENCES

ABRAMOWITZ, M. & STEGUN, I. A. 1965 *Handbook of Mathematical Functions*. Dover.

ALLEN, C. M. 1981 Numerical simulation of contaminant dispersion in estuary flows. (In preparation.)

ARIS, R. 1960 On the dispersion of a solute in pulsating flow through a tube. *Proc. R. Soc. Lond.* A **259**, 370–376.

BOWDEN, K. F. 1965 Horizontal mixing in the sea due to a shearing current. *J. Fluid Mech.* **21**, 83–95.

CHATWIN, P. C. 1970 The approach to normality of the concentration distribution of a solute in a solvent flowing along a straight pipe. *J. Fluid Mech.* **43**, 321–352.

CHATWIN, P. C. 1975 On the longitudinal dispersion of passive contaminant in oscillatory flow in tubes. *J. Fluid Mech.* **71**, 513–527.

ELDER, J. W. 1959 The dispersion of marked fluid in turbulent shear flow. *J. Fluid Mech.* **5**, 544–560.

FISCHER, H. B. 1972 Mass transport mechanisms in partially stratified estuaries. *J. Fluid Mech.* **53**, 671–687.

GILL, W. N. & SANKARASUBRAMANIAN, R. 1971 Dispersion of a non-uniform slug in time-dependent flow. *Proc. R. Soc. Lond.* A **322**, 101–117.

HOLLEY, E. R., HARLEMAN, D. R. F. & FISCHER, H. B. 1970 Dispersion in homogeneous estuary flow. *J. Hydraul. Div. A.S.C.E.* **96**, 703–724.

MAXEY, M. R. 1978 Aspects of unsteady turbulent shear flow. Ph.D. thesis, University of Cambridge.

POSMENTIER, E. S. 1977 The generation of salinity fine-structure by vertical diffusion. *J. Phys. Oceanog.* **7**, 298–300.

SMITH, R. 1976 Longitudinal dispersion of a buoyant contaminant in a shallow channel. *J. Fluid Mech.* **78**, 677–688.

SMITH, R. 1979 Calculation of shear-dispersion coefficients. In *Proc. Conf. on Mathematical Modelling of Turbulent Diffusion in the Environment, Liverpool, Sept.* 1978 (ed. C. J. Harris), pp. 343–362. Academic.

SMITH, R. 1981 A delay-diffusion description for contaminant dispersion. *J. Fluid Mech.* **105**, 469–486.

TALBOT, J. W. & TALBOT, G. A. 1974 Diffusion in shallow seas and in English coastal and estuarine waters. *Rapp. P.-v. Reun. Cons. Int. Explor. Mer.* **167**, 93–110.

TAYLOR, G. I. 1953 Dispersion of soluble matter in solvent flowing slowly through a tube. *Proc. R. Soc. Lond.* A **219**, 186–203.

THACKER, W. C. 1976 A solvable model of shear dispersion. *J. Phys. Oceanog.* **6**, 66–75.

YOTSUKURA, N., FISCHER, H. B. & SAYRE, W. W. 1970 Measurements of mixing characteristics of the Missouri River between Sioux City, Iowa and Plattsmouth, Nebraska. *U.S. Geol. Survey* no. 1899-G, Washington, D.C.